Understanding the 3D structure of the disk around LkHa330

PI: M. Benisty, U. de Chile

Scientific justification

General context. Observations of exoplanets revealed a wide diversity in the architectures of extrasolar systems which challenge our theories of planet formation. How do the physical conditions in protoplanetary disks, and their evolution with time, influence planet formation, is a fundamental question. While the direct detection of planets in an early phase of their formation, still embedded in disks, is extremely challenging, recent observations of these disks revolutionized our field and suggest that planet formation occur very early in the disk history. High resolution observations in both scattered light and millimeter regime, have shown a variety of small scale structures, such as rings and gaps (e.g. Fedele et al. 2018), spiral arms (e.g. Pérez et al. 2016; Benisty et al. 2015, 2017), and azimuthal asymmetries (Casassus et al., van der Marel et al.), that might indirectly trace embedded planets. These features have now been detected in both young and old disks (e.g. ALMA Partnership et al. 2015; Andrews et al. 2016), around low-mass (Pinilla et al. subm) and intermediate-mass stars (e.g. Isella et al. 2016), indicating that these features are an universal aspect of disk evolution.

Transition disks (TD) are key objects to investigate planet-disk interaction, as they show a large cavity with a dust depleted inner region (Andrews et al. 2011). The cavity and ring morphology observed at millimeter wavelengths can, for example, be explained by dust trapping in a pressure maximum. Such dust traps might be the key to planet formation, as they can retain dust grains and allow efficient growth to planetesimals, which would otherwise drift towards the star within very short timescales. These pressure maxima can for example be generated by a planet (Pinilla et al. 2012; Rosotti et al. 2016) or a vortex as a result of a Rossby wave instability, which would appear as an azimuthal asymmetry in the millimeter images (Regály et al. 2012; Birnstiel, et al. 2013). One additional striking discovery in recent observations of TD are the spiral arms in scattered light observations (Muto et al. 2012; Benisty et al. 2015, 2017) and in sub-millimeter gas tracers (Tang et al. 2017). The spirals have often similar morphologies: two symmetric arms with a pitch angle of about 15°–30°. One of the most exciting explanation of these features is that they are excited by one or more undetected companion(s) (Ogilvie & Lubow 2002), and spirals can therefore be signposts of planets embedded in the disk.

Despite being of fundamental importance for the global disk structure and the evolution of the disk-planet system, the temperature and density perturbations that spirals and vortices trace, remain unknown. The knowledge of the 3D structure of the disk would be a significant help to understand the physics of the spiral excitation mechanism and vortices. Reconstructing the 3D structure of the disk is possible by comparing the distributions of gas, small dust grains that are well coupled to the gas, and of large sized particles that are partly decoupled from the gas, settled to the midplane and possibly trapped. This however requires comparably high spatial resolution observations both in the near-infrared (probing the small dust in the upper layers of the disk), and sub-millimeter (probing the large grains in the disk mid-plane) regimes.

Target selection. Of particular interest is the disk around the young star LkHα330. Located at 250 pc, the disk, inclined by 35°, shows evidence for a large cavity in its spectral energy distribution and in images at millimeter wavelengths (Fig. 1; Brown et al. 2009; Andrews et al. 2011; Isella et al. 2013). The cavity is marginally resolved and shows strong azimuthal asymmetries. The asymmetry between the East and the West is about a factor of 2 in flux density in the CARMA 1.3 mm image, and possibly indicate dust trapping in a vortex (Fig. 1, upper panels). Our recent scattered light VLT/SPHERE image, that traces micron-sized grains on the disk surface, shows two clear asymmetric features (marginally detected in previous scattered light observations by Akiyama et al. (2016)), in addition to a ring located inside the millimeter cavity: a spiral arm in the East and a complex feature, that

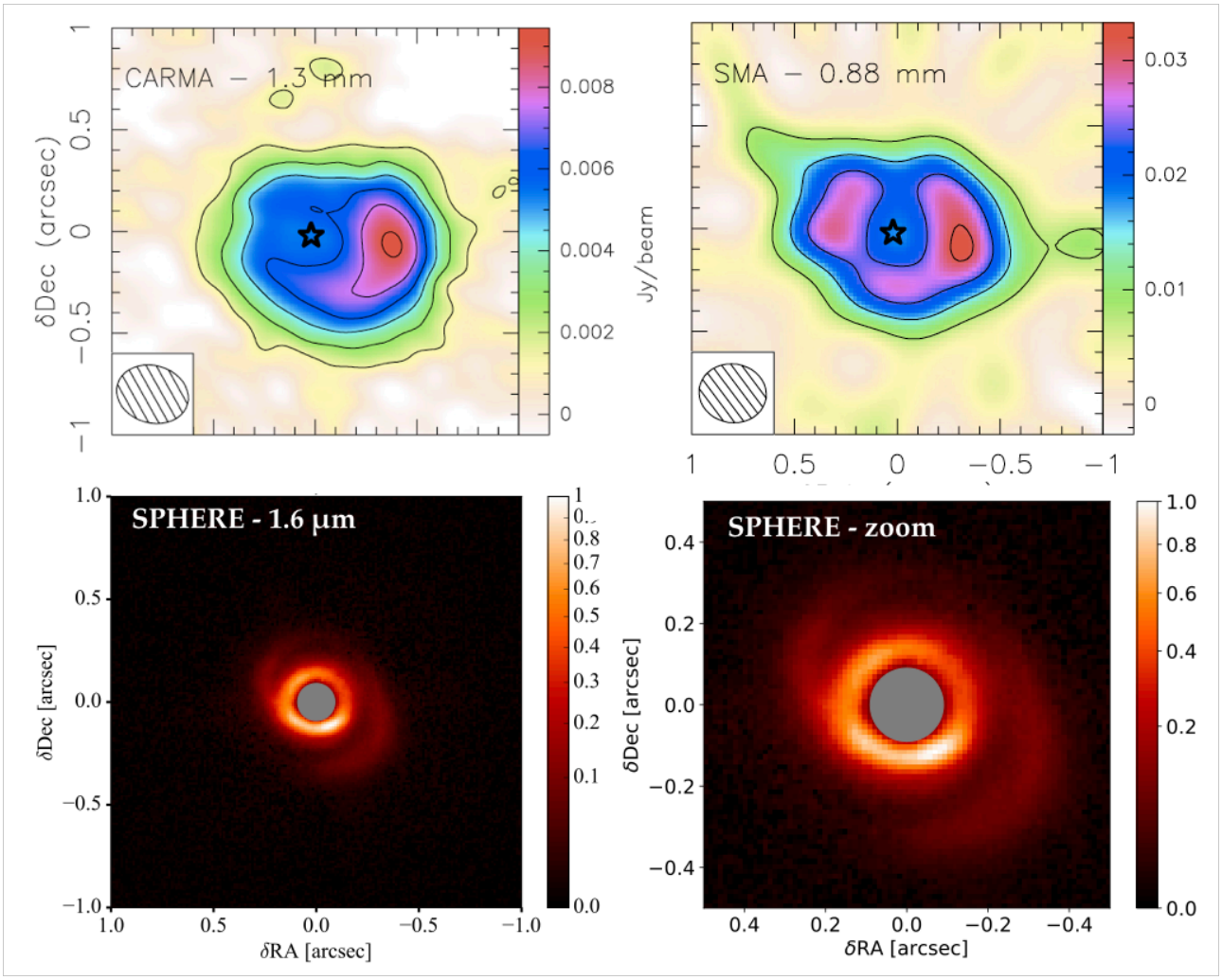

Figure 1: Top left and right: CARMA 1.3 mm and SMA 0.8 mm observations, respectively (Isella et al. 2013; Brown et al. 2009; Andrews et al. 2011). Both have a resolution of 0.35". Bottom left: NIR scattered light observations in H band showed at the same scale as the CARMA and SMA images. The grey mask is the coronagraph. Bottom right: zoom-in the SPHERE image (Benisty et al. in prep).

ressembles another spiral arm, in the West (Fig. 1, bottom panels). This feature could be constituted of a spiral arm and possibly tracing what is causing the millimeter asymmetry (Benisty et al. in prep). The limited sensitivity and resolution of both SMA and CARMA observations (0.35" resolution vs 0.04" for SPHERE) prevents a direct comparison of both tracers, and from understanding whether the asymmetry detected in the millimeter images are related to the features detected in scattered light. Unfortunately, no ALMA observations of LkHα330 with a resolution better than 0.8" exist.

Immediate observing goals

We propose to observe the disk around LkHα330, at high angular resolution (42 mas with C43-8), in Band 6, in the continuum and in the $J = 2 - 1$ transitions of CO, to constrain the 3D structure of the disk, and understand the nature of the features detected in the SMA, CARMA and SPHERE observations. We will determine whether the millimeter asymmetry is a vortex that trap particles, and if it is connected with the scattered light spirals (as in HD135344B, van der Marel et al. 2016). Besides the detection of the spirals in the sub-millimeter continuum and gas lines would make LkHα330 the first disk where spirals are unambiguously detected both in the surface layers and in the disk midplane.

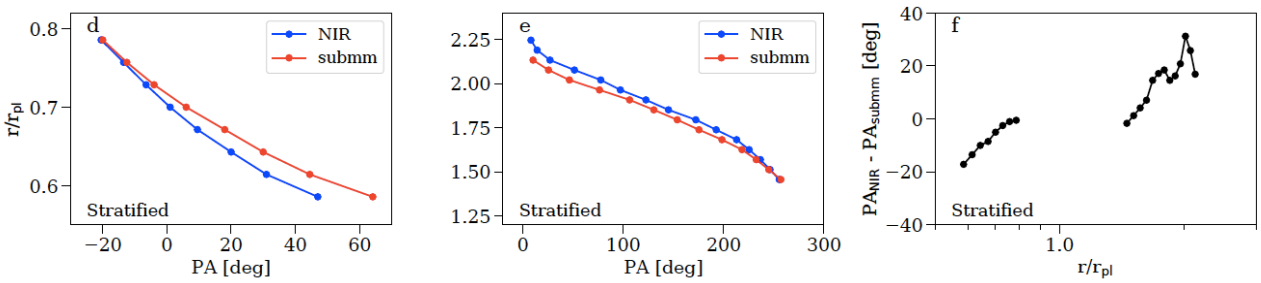

Figure 2: 3D planet-disk model predictions. Left and middle panels show the spiral wake from scattered light (blue) and sub-millimeter (red) synthetic maps, for the spiral arms located inwards of the companion (left) and outwards (middle). The spirals have different azimuthal positions in the warm upper layers of the disk (blue), than in the cold disk mid-plane (red). Right: the difference of the azimuthal position of the spirals in NIR and sub-millimeter decreases towards the position of the companion. The spatial resolution simulated is 0.04″. From Juhasz & Rosotti 2018.

In practice, we will be able to:

[1] Map the vertical temperature profile of the disk with the spirals.
Spirals density waves are constructive interference of sound waves excited at Lindblad resonances and their pitch angle depends on the local sound speed, which in turn depends on the temperature. Thus the pitch angle of spirals can be used as an indicator of the local gas temperature. Spirals become more open at higher gas temperatures, hence changes in the pitch angle between the scattered light spirals (on the surface layers) and the millimeter spirals (in the midplane) can be used to map the vertical variation of the temperature in the disk. Using 3D hydrodynamic and radiative transfer models, co-Is Juhasz & Rosotti showed that indeed spirals are more tightly wound in the cold disk mid-plane than in warm disk atmosphere and showed that the difference in pitch angle of the spirals is measurable with current instruments (Fig. 2 Juhász & Rosotti 2018). We will therefore use the Band 6 continuum to image the spiral wake in the disk mid-plane, at the same angular resolution as in the SPHERE image. We will then compare it to the spirals in scattered light image to measure the temperature variation between the disk mid-plane and the surface layers. To get an absolute measure of the temperature we will use the optically thick CO lines (^{12}CO and ^{13}CO) and provide temperature estimate of the disk atmosphere. We will then use these constraints in 3D hydrodynamic and radiative transfer models to understand the excitation of spirals in LkHα330 and constrain the location of the companion.

[2] Measure the density and thermal perturbations along the spirals.
While near-infrared scattered light images can provide us information on the density perturbations in the disk atmosphere, the optically thick lines (^{12}CO and ^{13}CO) can provide information on the thermal perturbations in the disk atmosphere along the spirals. Since the continuum emission in Band 6, and the C^{18}O line, are optically thin, the contrast of the spirals will be linearly proportional to both the density and the temperature variation.

[3] Determine the nature of the East/West asymmetry.
With the low resolution (0.35” corresponding to ∼90 au) of the previous millimeter observations, the cavity is marginally resolved, and although the flux ratio between the East and the West is clearly detected (factor ∼2 at 1.3 mm), the structure of the cavity, the disk inner rim and its asymmetries is unclear: is it an asymmetric ring? the signature of a spiral arm? or a vortex trapping dust grains? With the Band 6 continuum, at a resolution of ∼42 mas, we will gain a factor of ∼10 in resolution and distinguish the asymmetric features from the background disk.

To gain additional insight on the disk structure, we will study the kinematics of the three CO isotopologues available in band 6, which will allow us to detect departures from Keplerian rotation if a

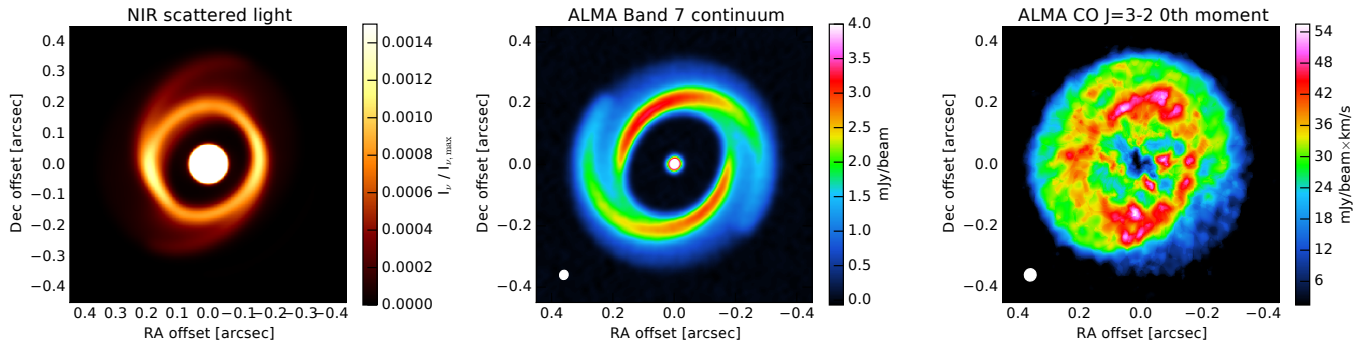

Figure 3: *Predicted signatures of surface density perturbation in the disk based on 3D radiative transfer calculations.*

massive body is located inside the cavity and responsible for the features.

Need for ALMA Cycle 6 and time estimate. Since the detected contrast between the spirals and the background disk depends on the spatial resolution, for a sensible comparison of the spirals in scattered light and in sub-millimeter, the ALMA observations require a resolution that matches that of scattered light images. To maximise the efficiency of our observations we chose Band 6 as it provides the highest S/N for the requested spatial resolution of ∼42 mas while simultaneously allowing to observe three CO isotopologues. The sensitivity estimate are based on the CARMA 1.3 mm observations. The peak of the disk is at 9.3 mJy/beam, while its opposite side is at 2.8 mJy/beam, within a 0.35”x0.35” beam.

[If I just take the CARMA estimate and divide by the beam area, I get a very long integration time. This doesn’t take into account that likely the flux will be concentrated in a narrower ring. I will aim for 20 microJansky as for the LP, which gives me 4 hours including 12CO and 13CO.]

[Looking at the SMA image, I wonder if I shouldn’t go for Band 7, even though it’s non standard?]

[Simulations: I could either show the great Figure 3 from Attila (band 7, so would need to change lambda). Or a toy model... or nothing.]

Team & Analysis tools: Our team consists of experts in observations of disks with scattered light imaging and sub-millimeter interferometry, and in modelling of protoplanetary disks, including dust evolution and trapping, spiral arms and vortices modelling. We will analyse and interpret the observations promptly with our models that include hydrodynamical, dust evolution, and radiative transfer calculations, and combine the ALMA and SPHERE observations for a multi-wavelength analysis.

References

Akiyama, E., Hashimoto, J., Liu, H. B., et al. 2016, AJ, 152, 222.

ALMA Partnership, Brogan, C., Pérez, L. M., et al. 2015, ApJL, 808, L3
Andrews, S., Rosenfeld, K., Wilner, D.& Bremer, M. 2011, ApJL, 742, 5
Andrews, S. M., Wilner, D. J., Zhu, Z., et al. 2016, ApJL, 820, L40
Benisty, M.; Juhasz, A.; Boccaletti, A. et al. 2015, A&A, 578, 6
Benisty, M.; Stolker, T.; Pohl, A. et al. 2017, A&A, 597, 42
Birnstiel, T., Dullemond, C. P. & Pinilla, P. 2013, A&A, 550, L8.

Brown, J. M., Blake, G. A., Qi, C., et al. 2009, ApJ, 704, 496.

Fedele, D., Tazzari, M., Booth, R., et al. 2018, A&A, 610, A24

Isella, A., Pérez, L. M., Carpenter, J. M., et al. 2013, ApJ, 775, 30.

Isella, A., Guidi, G., et al. 2016, Physical Review Letters, 117, 251101

Juhász, A. & Rosotti, G. P. 2018, MNRAS, 474, L32.

Muto, T., Grady, C. A., Hashimoto, J., et al. 2012, ApJ, 748, L22

Ogilvie, G. I. & Lubow, S. H. 2002, MNRAS, 330, 950.

Pérez, L. M., Carpenter, J. M., et al. 2016, Science, 353, 1519

Pérez, L. M., Carpenter, J. M., Chandler, C. J., et al. 2012, ApJ, 760, L17.

Pinilla, P., Benisty, M. & Birnstiel, T. 2012, A&A, 545, A81.

Regály, Z., Juhász, A., Sándor, Z., et al. 2012, MNRAS, 419, 1701.

Rosotti, G. P., Juhasz, A., Booth, R. A., et al. 2016, MNRAS, 459, 2790.

Tang, Y.-W., Guilloteau, S., Dutrey, A., et al. 2017, ApJ, 840, 32

Testi, L., Natta, A., Shepherd, D. S., et al. 2003, A&A, 403, 323.

van der Marel, N., Cazzoletti, P., Pinilla, P., et al. 2016, ApJ, 832, 178.